Surface Characterization of Hollow Fiber Membranes Used in Artificial Kidney

Mehrdad Rafat,[1] Dibyendu De,[2] K. C. Khulbe,[1] Thanh Nguyen,[2] Takeshi Matsuura[1]

[1]*Industrial Membrane Research Institute, Department of Chemical Engineering, University of Ottawa, Ottawa, Ontario K1N 6N5, Canada*
[2]*Research and Development, Baxter Healthcare Corporation, Miami Lakes, Florida 33014*

Received 18 February 2004; accepted 10 June 2005
DOI 10.1002/app.23052
Published online in Wiley InterScience (www.interscience.wiley.com).

ABSTRACT: The internal and external curved surfaces of polysulfone hollow fiber membranes were characterized by atomic force microscopy (AFM), contact angle measurement (CAM), and scanning electron microscopy (SEM) with the aim of improving the membrane surface properties for blood compatibility. Novel approaches were applied to evaluate a number of properties, including the roughness, pore size, nodule size, and wettability of the surfaces of the hollow fibers. CAM studies were carried out by directly observing the liquid meniscus at the surfaces of hollow fibers. Observation of the meniscus and measurement of the contact angle became possible by using an imaging system developed in our laboratory. AFM and SEM studies were also conducted on the surfaces of the hollow fiber membranes by cutting them at an inclined angle. The effect of the molecular weight of poly(ethylene glycol) (PEG) in the polymer blend on the surface properties of the hollow fibers was studied. Increasing the PEG molecular weight increased the average pore size whereas it decreased the contact angle. The contact angle depended on the microscopic surface morphology, including nodule size and roughness parameters. The theoretical prediction along with the experimental data showed that the measured contact angle would be greater than the value intrinsic to the membrane material because of the formation of composite surface structures. © 2006 Wiley Periodicals, Inc. J Appl Polym Sci 101: 4386–4400, 2006

Key words: atomic force microscopy; hollow fiber membranes; surfaces; polysulfone; contact angle measurement

INTRODUCTION

One of the most important applications of membrane technologies is hemodialysis in which membranes are used as artificial kidneys.[1] The main requirement for hemodialysis membranes is biocompatibility, which is influenced by both membrane material and membrane surface properties. It has been reported that membranes with smoother surfaces have better blood compatibility.[2] In addition, several studies have indicated that the interfacial interactions between the biological environment and biomaterial are mediated by the membrane surface properties such as hydrophilicity and hydrophobicity, electrostatic attraction, surface composition, and so forth.[3,4]

In recent years, many surface-sensitive techniques such as atomic force microscopy (AFM), contact angle measurement (CAM), X-ray photoelectron spectroscopy, and scanning electron microscopy (SEM) have been developed to analyze polymeric surfaces.[5] Among these techniques, only a few have been applied to the internal blood-contacting surfaces of hollow fibers for dialysis.

In the course of this research, three techniques were applied for the characterization of the internal and external surfaces of dialysis hollow fibers: CAM, AFM, and SEM. Despite the popularity and maturity of these techniques, they were not all successfully applied to the inside and outside surfaces of polysulfone dialysis hollow fibers.[6] This was because of difficulties introduced by the surface curvature, small size, and low transparency of polysulfone hollow fibers. The hollow fibers studied in this work were melt-spun polysulfone hollow fiber membranes with an average inside diameter of 200 μm and an average wall thickness of 10 μm. The hollow fiber membranes were manufactured from a synthetic high performance polymer via the thermally induced phase separation (TIPS) process. Unlike solution spinning, the polysulfone melt was extruded through a spinneret at an elevated temperature and then cooled by air to create the membrane.[7] In the TIPS process, the polymer and plasticizers were mixed together at a high temperature to form a homogeneous melt, which is also called dope. This dope was then extruded through a spinneret with nitrogen gas in the core to create a hollow fiber. Cooling of the fiber was done gradually along the length, thereby controlling the membrane structure. This cre-

Correspondence to: T. Matsuura (matsuura@eng.uottawa.ca).
Contract grant sponsor: Government of Ontario, Canada, Ontario Graduate Scholarship in Science and Technology.

ates a membrane having a uniform microporous wall structure with a very smooth inner surface. Only heat exchange was used in this process; that is, there were no chemicals or additives added in the fiber lumen for the creation of the microstructure as in solution spinning.[8]

The objectives of this study were threefold:

1. to apply surface characterization techniques such as CAM, AFM, and SEM to the internal and external surfaces of dialysis hollow fiber membranes;
2. to study the hollow fiber membranes' internal and external surface properties such as the pore size, pore size distribution, nodule size, nodule size distribution, roughness, and wetting properties in order to develop novel hollow fibers with long-term biocompatibility and high performance; and
3. to develop a theory capable of predicting the effect of membrane morphology on surface energy.

CAM, AFM, and SEM are applicable to the internal and external surfaces of dialysis hollow fibers and valuable surface information can be obtained by combining these techniques, especially CAM and AFM. For example, we found that the surface hydrophilicity was dependent on the combination of the membrane surface nodule size and roughness: membranes with smaller nodules and rougher surfaces had higher contact angles compared to those with larger nodules and smoother surfaces. A theoretical model capable of predicting the effect of composite structures on the contact angle was also developed.

THEORETICAL

The effect of the surface nodule size and roughness on the wettability of hollow fiber membranes was studied. Young's equation was examined and modified. In particular, our study on the effect of nodule size and roughness on the membrane surface is based on the concept that liquid cannot completely fill the troughs created between the nodules. The smaller the nodules and rougher the surface are, the less the liquid penetrates into the troughs. In this case, the surface is considered as a composite surface in which the liquid does not come in complete contact with the solid surface because of the air trapped in the troughs. Therefore, there is a decrease in the effective area of contact between the liquid and solid, causing the increase in the membrane surface contact angle (see Fig. 1).

The well-known Young's equation for a contact angle on an ideal (smooth, homogeneous, rigid) surface may be written in the following form:

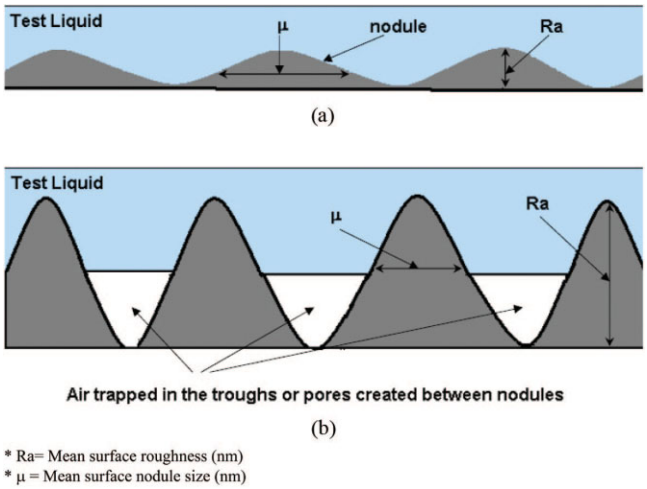

Figure 1 Cross-sectional drawings of relatively (a) smooth and (b) rough composite surfaces.

$$\cos\theta_i = (\gamma_{SV} - \gamma_{SL})/\gamma_{LV} \quad (1)$$

where γ is the surface tension (or surface free energy); θ_i is the intrinsic contact angle; and the subscripts SV, SL, and LV refer to the solid–vapor, solid–liquid, and liquid–vapor interfaces, respectively.[9]

In the case of a composite surface described in Figure 1, the following modified form of Young's equation is proposed to consider the effect of trapped air in the troughs:

$$\cos\theta_a = (\gamma_{SV} - \gamma_{SLE})/\gamma_{LV} \quad (2)$$

where θ_a is the apparent contact angle and γ_{SLE} is the effective surface tension for a solid–liquid system, which is defined by eq. (3):

$$\gamma_{SLE} = \gamma_{SL} \cdot f_{SL} + \gamma_{LV} \cdot f_{LV} \quad (3)$$

where f_{SL} is the fraction of the surface where the solid and liquid are in contact and f_{LV} is the fraction of the surface where the liquid and vapor (air) are in contact.

Equation (4) can be derived by combining eqs. (1), (2), and (3):

$$\cos\theta_a = \cos\theta_i - f_{LV}(1 - \gamma_{SL}/\gamma_{LV}) \quad (4)$$

Equation (4) implies that θ_a will become more than θ_i when $\gamma_{SL} < \gamma_{LV}$ and f_{LV} increases. When the test liquid is water, γ_{LV} is known to be 72.8×10^{-3} J/m^2. In addition, the value of γ_{SL} is reported to be 31.3×10^{-3} J/m^2 for polysulfone material.[10]

Moreover, comparing Figure 1(a,b), as the ratio of the mean surface roughness to the mean surface nodule size (R_a/μ_n) increases, it is evident that the chance of air being trapped in the troughs increases because of the capillary effect, which further leads to an in-

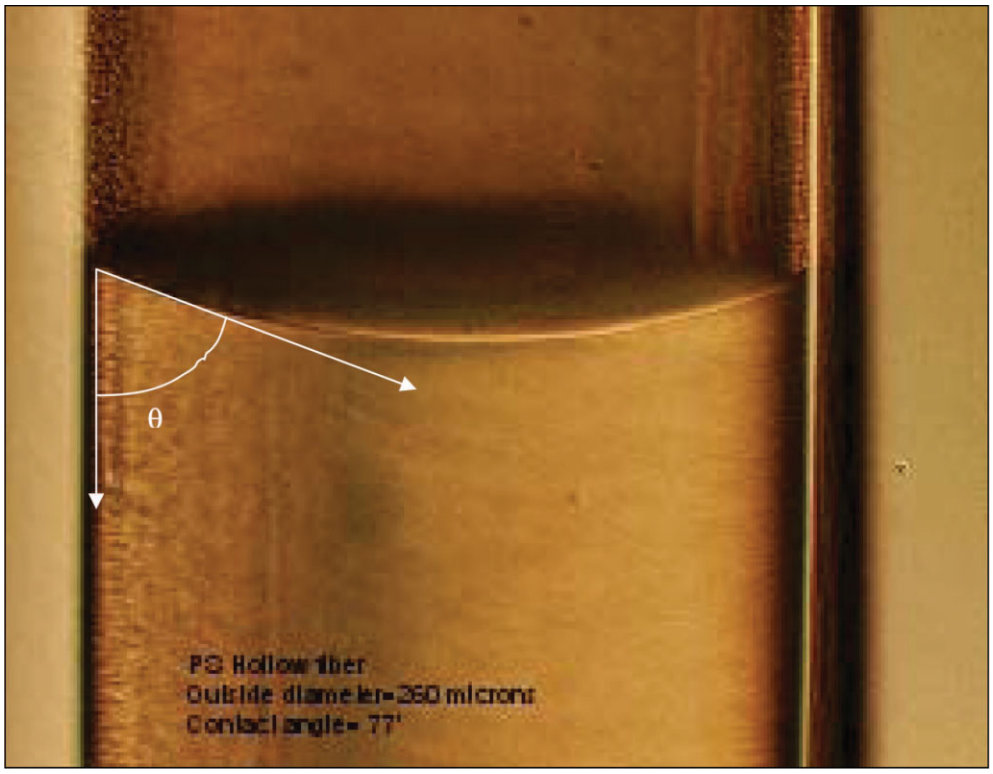

Figure 2 The internal meniscus of polysulfone dialysis hollow fiber membranes.

crease in $f_{LV.}$ Therefore, θ_a becomes greater than θ_i. This means that the contact angle of the composite surfaces becomes greater than the value intrinsic to the material and increases with an increase in R_a/μ_n when $\gamma_{SL} < \gamma_{LV}$. This is confirmed in the Experimental section.

EXPERIMENTAL

Materials

Melt-spun polysulfone hollow fiber membranes were manufactured from a synthetic high performance polymer via the TIPS process. The polymer solution included 25% polysulfone (bisphenol A) and 45% solvent (Sulfolane). Then, the nonsolvent, poly(ethylene glycol) (PEG), was fixed at 30%.[7] The polymer solution was then extruded through a spinneret with nitrogen gas in the core to create a hollow fiber.

As per procedure, some of the hollow fibers were dried in an oven at 70°C for predetermined periods after leaching out solvents and nonsolvents. In addition, all fibers were manufactured by blending polysulfone with different molecular weights of PEG (1000, 1500, and 2000 Da).

Methods

CAMs

Experimental apparatus. CAM was carried out by goniometrical determination of the angle from observations of the three-phase meniscus system (see Fig. 2). For this purpose, a hollow fiber goniometer was developed in our laboratory by combining a wetometer (model 104, Rame–Hart) with an NRL C.A. goniometer (model 100, Rame–Hart, see Fig. 3). In order to increase the magnification ratio of the hollow fiber goniometer, the existing objective lens was replaced with two lenses that had higher magnification ratios (Olympus models IC-10 and IC-20). The IC-10 lens was used for the measurements at the internal surfaces whereas the IC-20 was used for the measurements at the external surfaces.

The gonimeter eyepiece was replaced with an eyepiece (Olympus model WHK 10×/20 L-H) equipped with a 360° protractor (Olympus model NE45), a pattern diameter of 10 mm, and a graticule size of 20.4 mm. In addition to the above modifications, two fiber optic illuminators were attached to the system to clearly monitor the meniscus.

Sample preparation. Glycerin was used to preserve the membrane pore structure prior to drying of the membrane, so the first step was to remove it from the surface of the hollow fiber membranes. The hollow fibers were placed in a perforated vessel that was dipped into a beaker containing distilled water. A laboratory stirrer and a magnetic stir bar were used to circulate water in the vessel for 0.5 h. After glycerin removal, the fibers were dried in air for 1 h. Then, they were cut into 20 cm long fibers. Each piece of hollow

Figure 3 A hollow fiber goniometer developed by combining an NRL Rame–Hart model 100 contact angle goniometer with a Rame–Hart, model 104 wetometer.

fiber was gently mounted on a rectangular metallic frame by double-sided tape at the top and bottom.

Measurement technique. The technique used in this study (meniscus technique) is a novel approach toward the direct measurement of the contact angles at the internal and external surfaces of dialysis hollow fiber membranes. The main advantage of this technique is its straightforwardness. Whereas this technique provides useful information on both the wettability and surface morphology of the membrane, the previously used techniques (Wilhelmy plate and capillary rise techniques) provide some information on the membrane wettability without taking the surface morphology of the material into account.

In this technique, each metal-frame mounted hollow fiber was partially immersed in the test liquid (distilled water). Then, the capillary rise and meniscus at the interior and exterior of the hollow fiber were monitored by the hollow fiber goniometer.

The equilibrium contact angle was measured after the equilibrium condition was reached (see Fig. 2). Advancing and receding contact angles were also measured by gradually increasing and decreasing the level of the test liquid in the container in which the hollow fiber was partially immersed. Each contact angle was the average of at least seven measurements. In all cases, the contact angle data were reported in terms of the equilibrium contact angle (θ_e), unless otherwise specified.

AFM studies

AFM experimental apparatus. AFM studies were conducted in tapping mode at the interior and exterior of the hollow fibers using a Nanoscope III equipped with a 1553D scanner (Digital Instruments, CA). A crystal silicon probe cantilever was used, which had a spring constant of 20–100 Nm^{-1}, length of 125 μm, and nominal tip radius of curvature of 5–10 nm.

Sample preparation. It became possible to access the internal surface of the hollow fibers by cutting them at an inclined angle. Each hollow fiber was cut in a small piece of 1-cm length, which was fixed to a metal disk (a puck, 1.5-cm outer diameter) by double-sided tape. Then, the hollow fiber was cut at an inclined angle by a sharp razor under a microscope as shown in Figure 4.

AFM analysis technique. During this study, the roughness parameters were determined by the AFM software and the pore size and nodule size were determined by visual inspection of the line profile of different pores and nodules from various AFM images (see Fig. 5). The membrane surface morphology was also expressed in terms of the R_a, μ_n, and mean surface pore size (μ_p). The mean roughness is the mean value of the surface relative to the center plane, the plane for which the volume enclosed by the image above and below this plane are equal, and it is calculated as

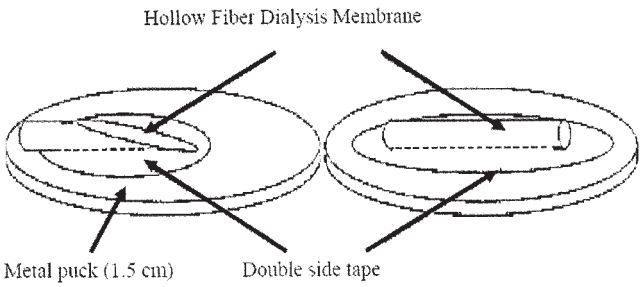

Figure 4 The cutting technique used for AFM studies of the internal surface of dialysis hollow fiber membranes.

$$R_a = \frac{1}{L_x L_y}\int_0^{L_y}\int_0^{L_x} |f(x,y)|dxdy \qquad (5)$$

where $f(x, y)$ is the surface relative to the center plane and L_x and L_y are the dimensions of the surface in the respective x and y directions.[11]

Figure 5 represents the cross-sectional view of the nodules and pores and the measurement of these parameters from AFM. Measurements of nodules and pores were taken from cross-sectional views of the data along the reference line. For a pair of cursors, the horizontal distance represents the diameter of a nodule or a pore. The mean diameter of a pore or a nodule is based on at least 30 measurements. The scan size of each sample was 2 μm^2.

SEM studies

Micrographs of the cross-sectional internal and external surfaces of dialysis polysulfone hollow fibers were obtained using a scanning electron microscope (JEOL JSM 6400) composed of an X-Ray analyzer (Link eXL LZ4), Cryo-stage system (Oxford CT 1500), two backscatter detectors (Robinson and JEOL), and Tungsten and LaB6 filaments. Detailed delineation of the SEM experimental aspects are discussed elsewhere.[12] The same cutting technique used for AFM samples was used for SEM imaging in order to access the internal surfaces of the hollow fibers.

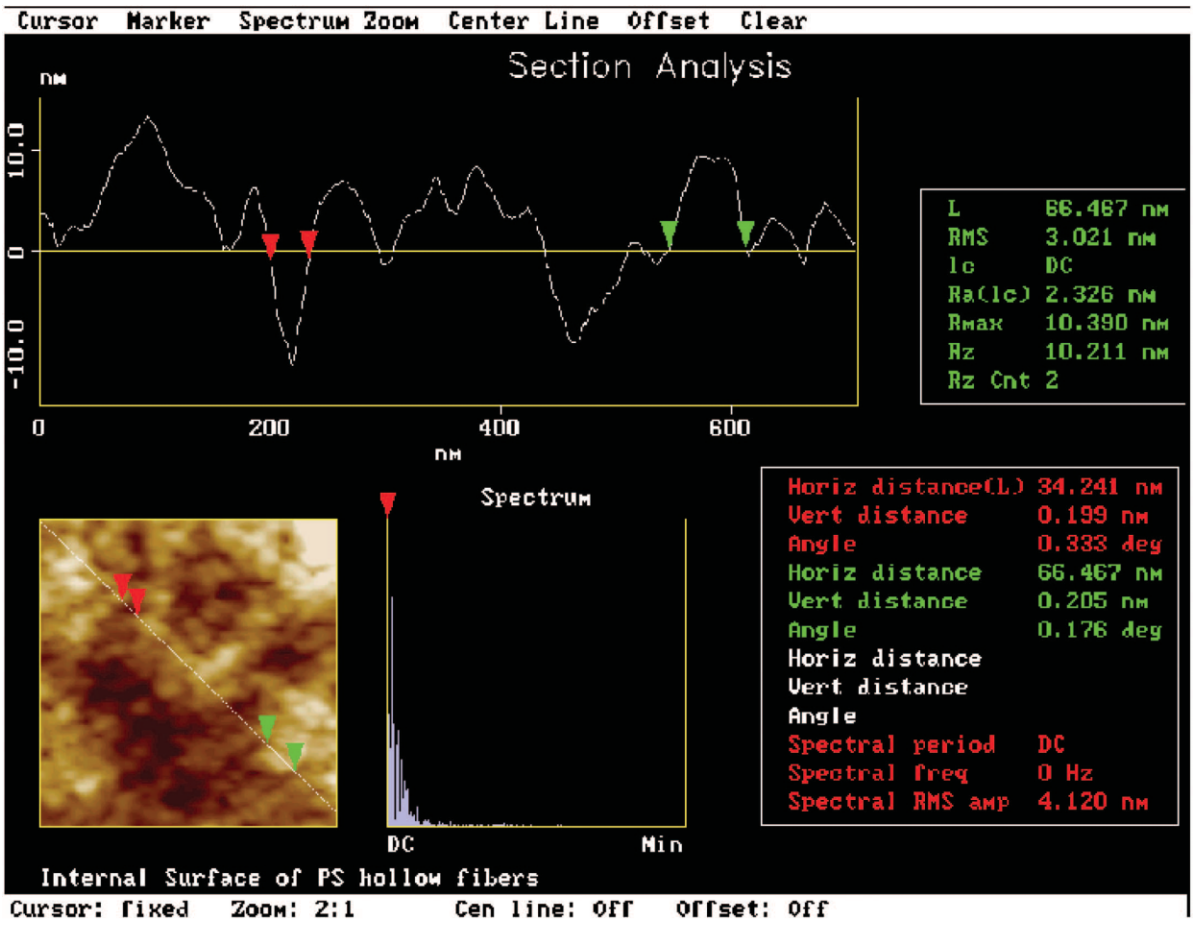

Figure 5 A cross-sectional view of nodules and pores at the internal surface of a polysulfone dialysis hollow fiber and the measurement of the nodule and pore sizes from AFM.

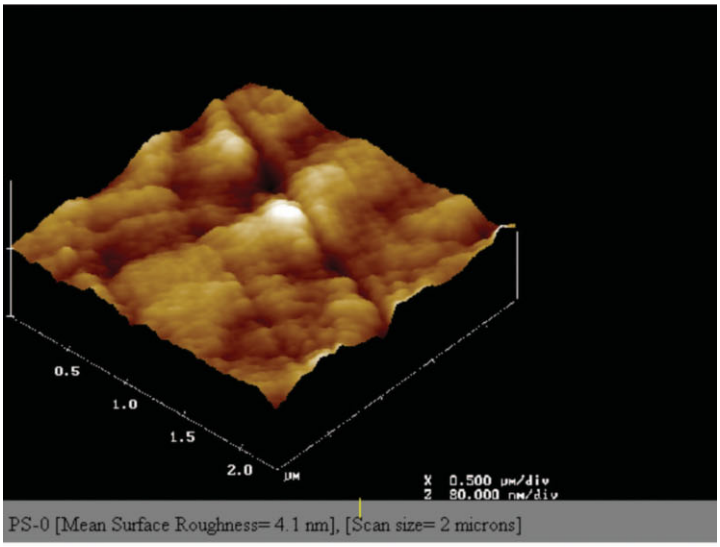

(a)

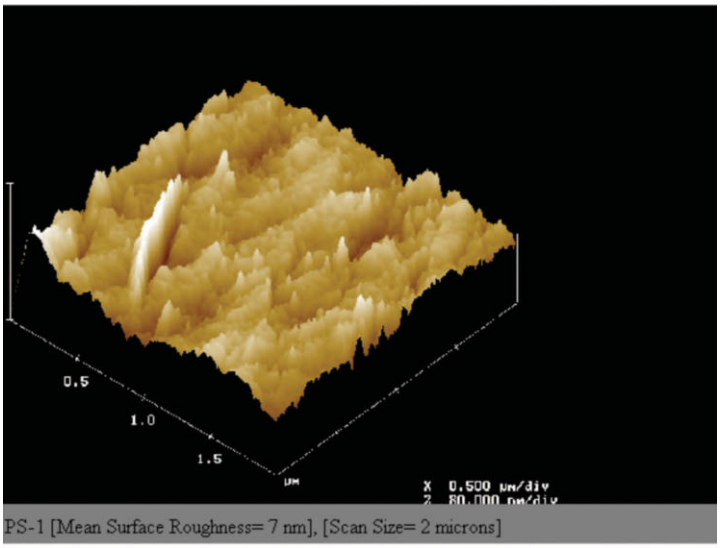

(b)

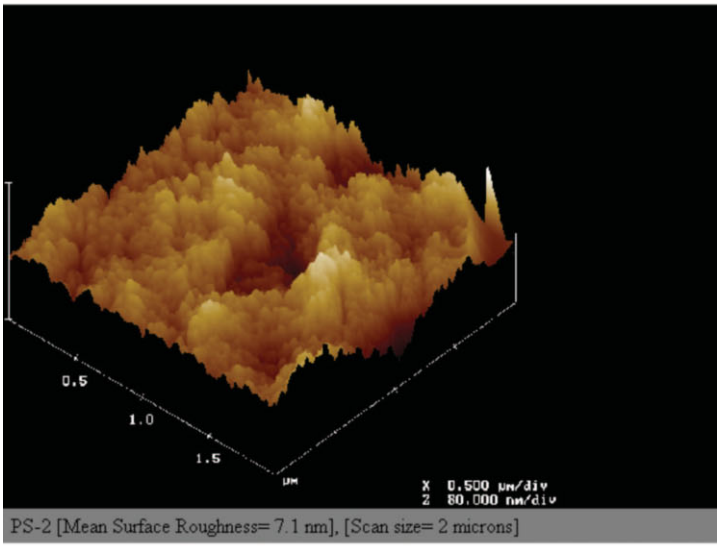

(c)

Figure 6 AFM images of the internal surfaces of polysulfone hollow fibers (a) PS-0 dried for 5 min, (b) PS-1 dried for 1 h, and (c) PS-2 dried for 2 h.

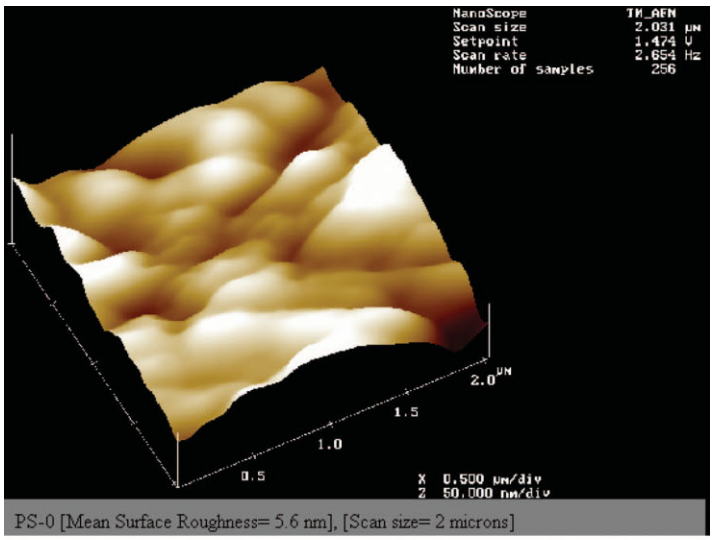

(a)

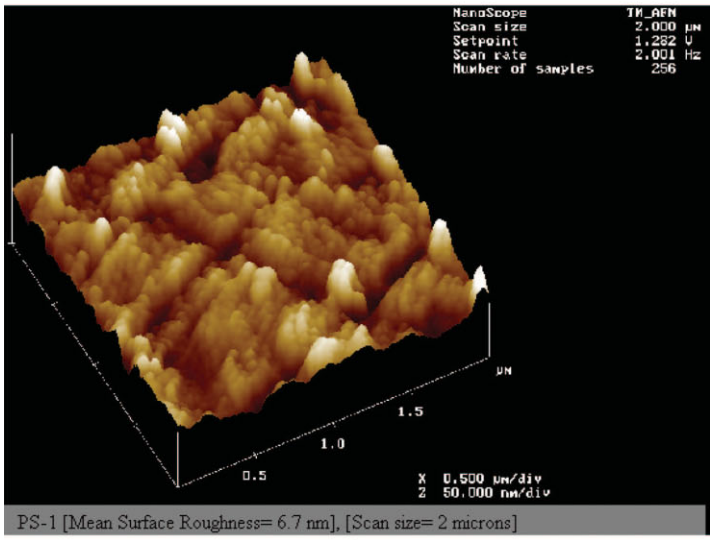

(b)

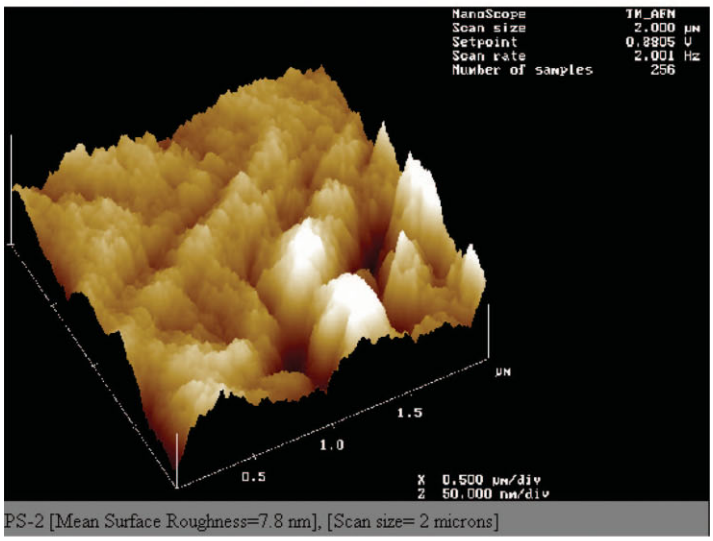

(c)

Figure 7 AFM images of the external surfaces of polysulfone hollow fibers (a) PS-0 dried for 5 min, (b) PS-1 dried for 1 h, and (c) PS-2 dried for 2 h.

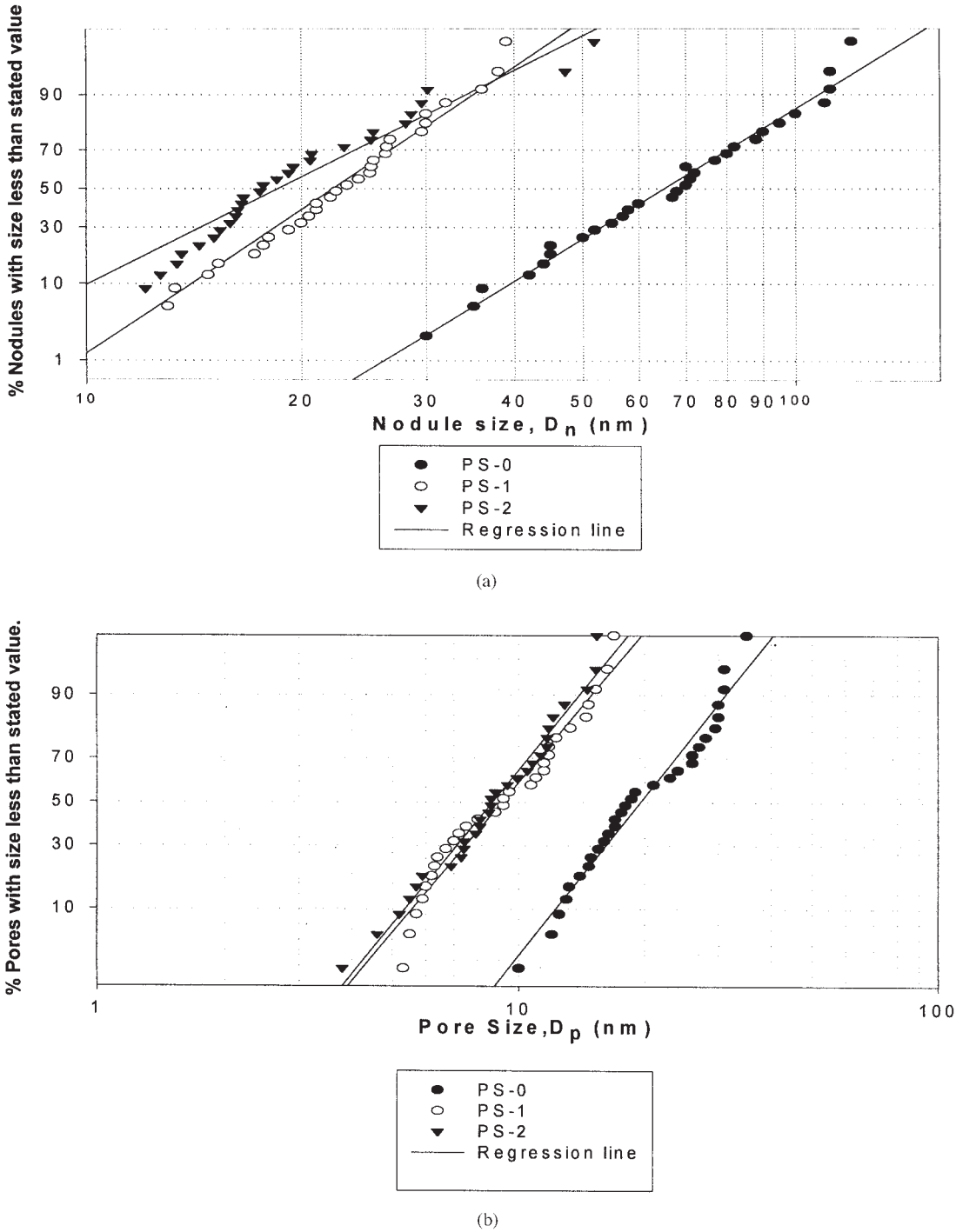

Figure 8 The log-normal distribution of (a) nodules and (b) pores at the internal surfaces of polysulfone hollow fibers PS-0, PS-1, and PS-2 subjected to drying for 5 min, 1 h, and 2 h, respectively.

RESULTS AND DISCUSSION

Effect of drying time on surface morphology

The internal and external surfaces of polysulfone hollow fibers blended with PEG with a molecular weight of 1000 Da were studied by AFM and CAM. Figures 6 and 7 represent the AFM images obtained from the internal and external surfaces of polysulfone hollow fibers, respectively. PS-0 hollow fiber was dried for a very short period of 5 min whereas PS-1 and PS-2 hollow fibers were dried for 1 and 2 h, respectively.

The membrane surface morphology is expressed in terms of three parameters: R_a, μ_n, and μ_p. Nodule sizes and pore sizes were measured at the inside and outside surface of the hollow fibers by visual inspection of line profiles of different nodules and pores from var-

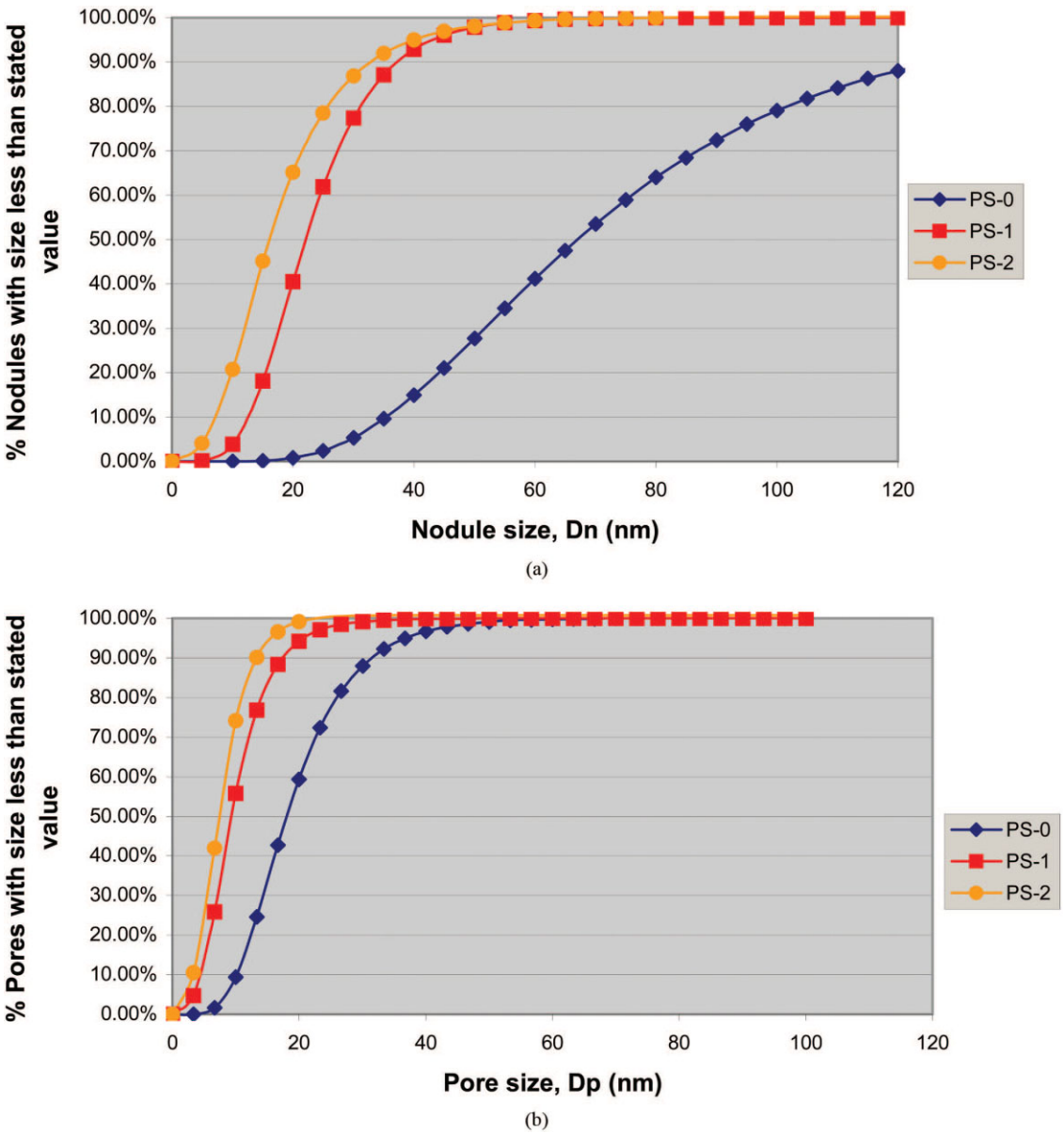

Figure 9 Cumulative size distributions of (a) the internal surface nodules and (b) the internal surface pores of polysulfone hollow fiber membranes PS-0, PS-1, and PS-2 subjected to drying for 5 min, 1 h, and 2 h, respectively.

ious AFM images. The results were arranged in ascending order and assigned median ranks. To obtain a distribution function graph, these median ranks were plotted on the ordinate (y axis) against the nodule or pore sizes arranged in an increasing order on the abscissa (x axis, see Fig. 8). This plot yields a straight line on a log-normal probability paper if the nodule size or pore size measurements have a log-normal distribution. From this plot the values of μ_n or μ_p and geometric standard deviations of the nodule (σ_n) or pore (σ_p) sizes can be calculated.[11]

In addition to log-normal distribution charts, cumulative nodule size and pore size distribution (see Fig. 9) and probability density function curves (see Fig. 10) were generated based on the mean values and standard deviations for nodule sizes and pore sizes. The pore size (D_p) and nodule size (D_n) distribution of an ultrafiltration membrane can be expressed by the following probability density function[11]: Set

$$\frac{df(D_p)}{d(D_p)} = \frac{1}{\sqrt{2\pi}D_p \ln\sigma_p} \exp\left[-\frac{(\ln D_p - \ln\mu_p)^2}{2(\ln\sigma_p)^2}\right] \quad (6)$$

According to Singh et al.,[11] the pore sizes measured by AFM corresponded to the pore entrances, which were funnel shaped and had a maximum opening at the entrance, whereas the pore sizes obtained from a solute separation corresponded to a minimal sized pore constriction experienced by the solute while

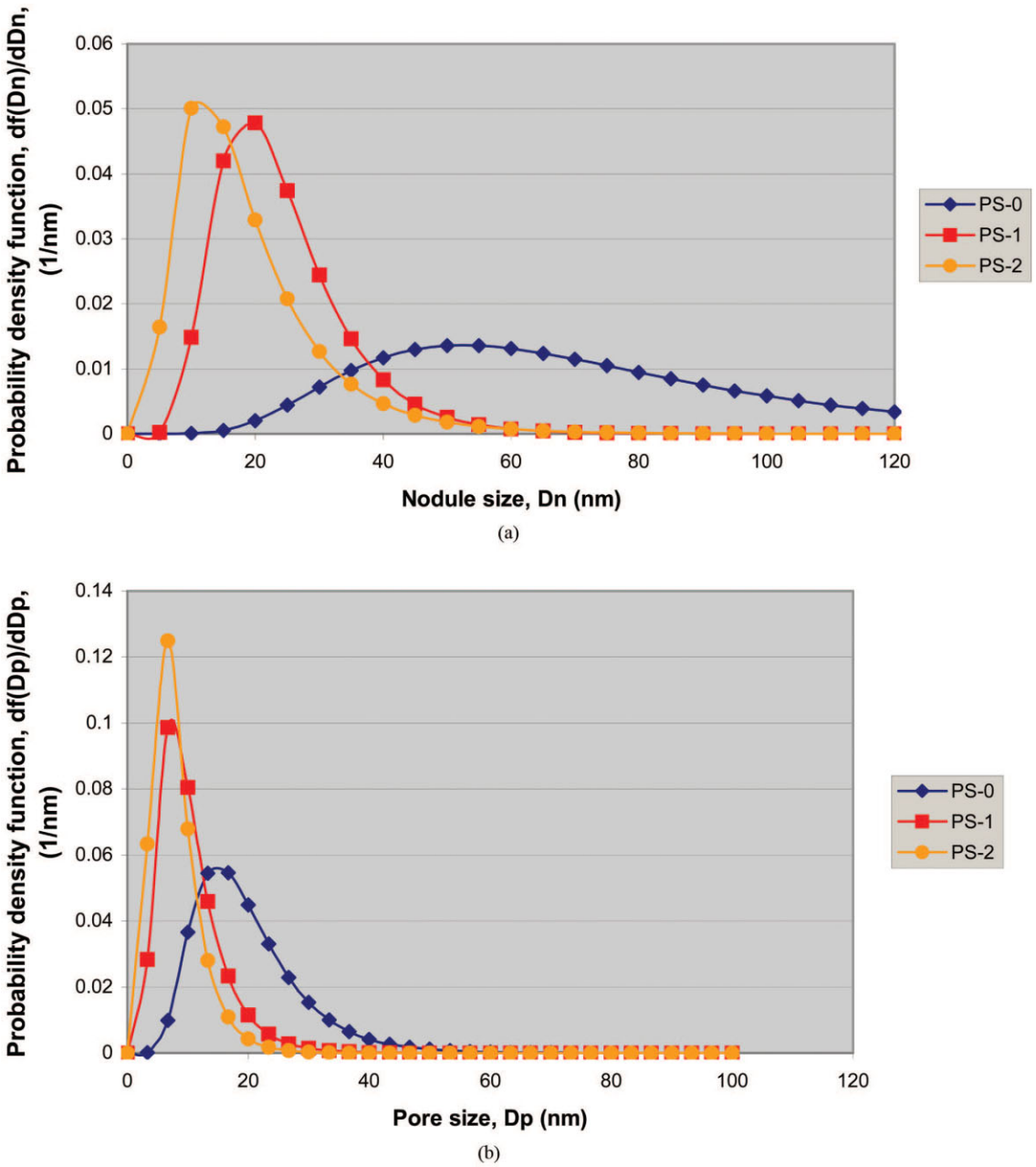

Figure 10 Probability density function curves generated for (a) the internal surface nodules and (b) the internal surface pores of polysulfone hollow fiber membranes PS-0, PS-1, and PS-2 subjected to drying for 5 min, 1 h, and 2 h, respectively.

TABLE I
Experimental Results of Surface Morphology and Contact Angle Measurement for Internal Surfaces of PS-0, PS-1, and PS-2 Hollow Fibers

Hollow fiber name	Drying time (h)	R_a (nm)	μ_n (nm)	μ_p (nm)	θ_e (°)
PS-0	0.08	4.1	67.0 ± 1.6	18.0 ± 1.4	77.0 ± 1.0
PS-1	1	7.0	22.0 ± 1.5	9.2 ± 1.6	81.2 ± 1.2
PS-2	2	7.1	16.0 ± 1.7	7.3 ± 1.6	82.0 ± 1.1

The PEG weight-average molecular weight in the polymer solution is 1000 Da.

TABLE II
Experimental Results of Surface Morphology and Contact Angle Measurement for External Surfaces of PS-0, PS-1, and PS-2 Hollow Fibers

Hollow fiber name	Drying time	R_a (nm)	μ_n (nm)	μ_p (nm)	θ_e (°)
PS-0	0.08	5.6	70.0 ± 1.6	39.0 ± 1.6	68.5 ± 1.4
PS-1	1	6.7	25.0 ± 1.5	6.7 ± 1.5	76.3 ± 3
PS-2	2	7.8	17.0 ± 1.75	6.2 ± 1.7	78.9 ± 2.5

The PEG weight-average molecular weight in the polymer solution is 1000 Da.

passing through the pore. Therefore, the pore sizes measured by AFM are normally larger than those obtained from a solute separation test, which are likely the real pore sizes of the membrane.

The experimental results of the surface morphology and CAM for polysulfone hollow fibers are summarized in Tables I and II for the internal and external surfaces, respectively.

Among the polysulfone hollow fibers, PS-0 that was dried for shorter time had the largest μ_n and μ_p but it had the lowest contact angle. In general, we found that the contact angle and roughness increased whereas both the nodule size and pore size decreased from PS-0 to PS-1 but they almost leveled off at PS-1.

Effect of membrane surface nodule size and roughness on contact angle

Figure 11 shows the measured and theoretical values of the equilibrium contact angle (θ_e) at the internal surface of five polysulfone hollow fibers as a function of the roughness and nodule size. The roughness and nodule size are combined and shown in the form of a single parameter k, which is the R_a/μ_n of the membranes. To obtain the values of the apparent contact angle from eq. (4), parameters f_{SL} and f_{LV} were assumed to be equivalent to the numerical values of $\mu_n/(\mu_n + \mu_p)$ and $\mu_p/(\mu_n + \mu_p)$, respectively. Figure 11 shows that the experimental values are in good agreement with the theoretical ones for the contact angle and both show the same trend when they are plotted against the k values.

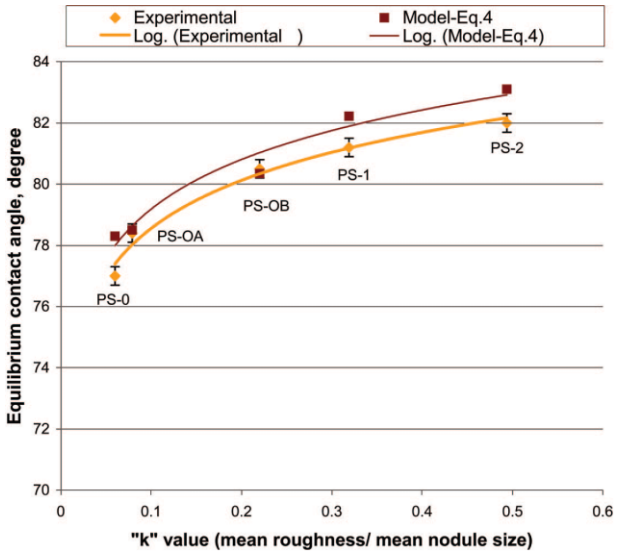

Figure 11 Experimental and theoretical equilibrium contact angles at the internal surfaces of PS-0, PS-0A, PS-0B, PS-1, and PS-2 hollow fibers versus the k value. (PS-0, PS-0A, and PS-0B are polysulfone hollow fibers dried for 5 min but manufactured under different spinning conditions.)

According to the data in Tables I and II and the graph shown in Figure 11, we found that membranes with a rougher surface and smaller nodules had a higher contact angle compared to those with a smoother surface and larger nodules as predicted in the Theoretical section. To explain the increase in the contact angle with the changes in the surface morphology, it was proposed that as the membrane surface nodule size decreases and the roughness increases, it becomes possible for the system to assume configurations in which the liquid does not completely penetrate into the troughs. The smaller the nodules and rougher the surface are, the narrower and deeper the troughs in which less liquid can penetrate because of the capillary effect.[13]

Effect of molecular weight of PEG blended in polymer solution on surface properties of hollow fibers

The surface properties of polysulfone hollow fibers manufactured from the polymer solutions blended with different molecular weight PEGs were investigated by AFM and CAM. Figure 12 shows the AFM images obtained from the internal surfaces of these polysulfone dialysis hollow fibers. Some of the AFM and CAM experimental results are also summarized in Table III.

Table III shows that blending of higher molecular weight PEG decreases the contact angle. Indeed, the decrease in the contact angle for PG-1500 and PG-2000 hollow fibers is due to the presence of higher molecular weight PEG chains in the membrane structure and surface. It was also observed from AFM images

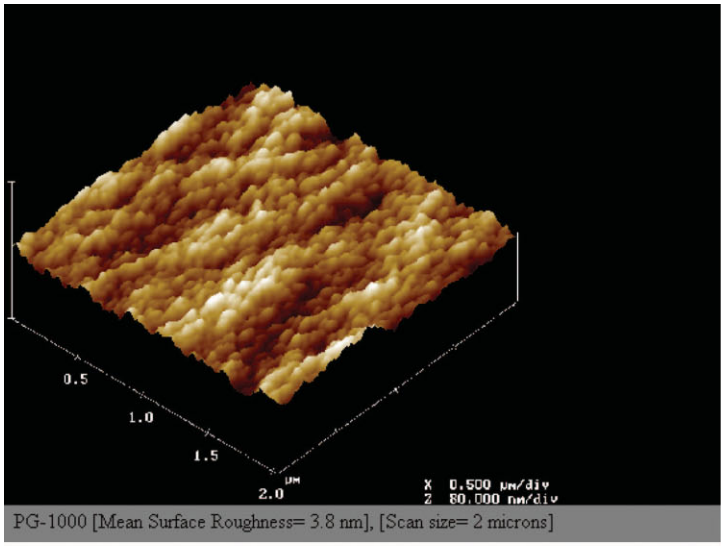

(a)

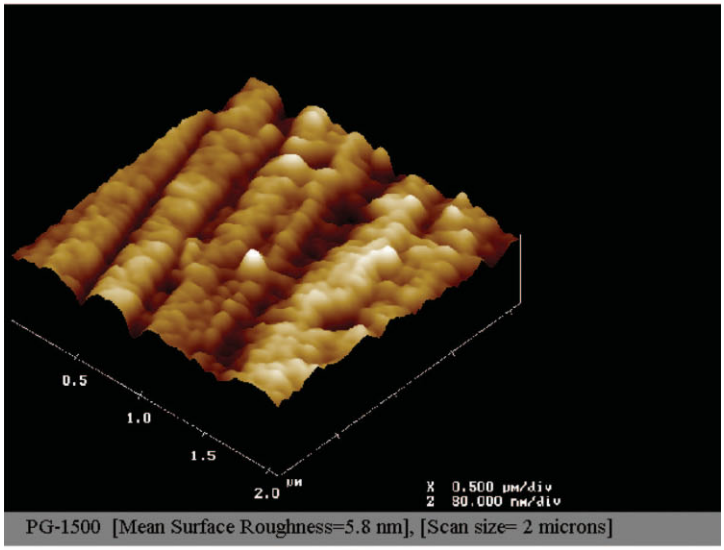

(b)

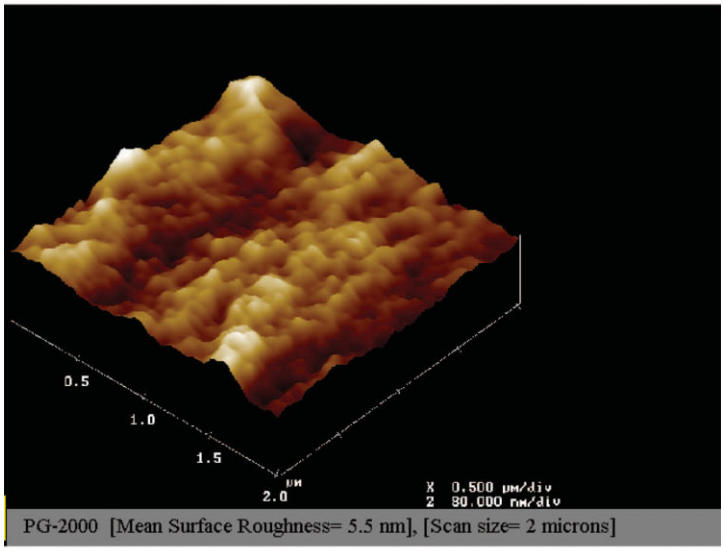

(c)

Figure 12 AFM images obtained from the internal surfaces of PG-1000, PG-1500, and PG-2000 dialysis hollow fibers synthesized from polymer solutions blended with PEG with molecular weights of 1000, 1500, and 2000 Da, respectively. PG-1000 is similar to the PS-0 hollow fiber but with a higher polymer concentration of 4%.

TABLE III
Experimental Results of Surface Morphology and Contact Angle Measurement for Internal Surfaces of PG-1000, PG-1500, and PG-2000 Polysulfone Hollow Fibers

Hollow fiber name	PEG M_w in polymer solution (Da)	R_a (nm)	μ_n (nm)	μ_p (nm)	θ_c (°)
PG-1000	1000	3.8	48.1 ± 1.4	9.2 ± 1.3	78.4 ± 1.2
PG-1500	1500	5.8	61.4 ± 1.3	15.4 ± 1.2	74.3 ± 1.4
PG-2000	2000	5.5	78.0 ± 1.4	17.9 ± 1.3	73.8 ± 1.0

The drying time is 5 min (0.08 h); M_w, weight-average molecular weight.

that the surface nodules were larger and aligned along the spinning direction for PG-1500 and PG-2000 compared to PG-1000.

Microstructure study of polysulfone dialysis hollow fibers by SEM

The microstructure of the polysulfone hollow fibers was investigated by SEM. There was an ultrathin skin on both the inner and outer surfaces. Although the ultrathin inner surface offers good possibilities for solutes to permeate through the membrane because of the low resistance, the outer thin layer serves as an excellent barrier to endoxins.[8] Figure 13 illustrates the skin layers at the internal and external surfaces of a typical polysulfone hollow fiber used in this study.

The effect of the drying time or duration on the surface of the membranes was also studied by SEM. The SEM images obtained from the external surface of the hollow fibers showed that the membrane surfaces were affected by the drying duration. Figure 14 presents the external surfaces of polysulfone hollow fibers dried for 5 min or 1 h. Fissures and cleavages within a size range of 1–3 μm were produced as the effect of a longer drying period.

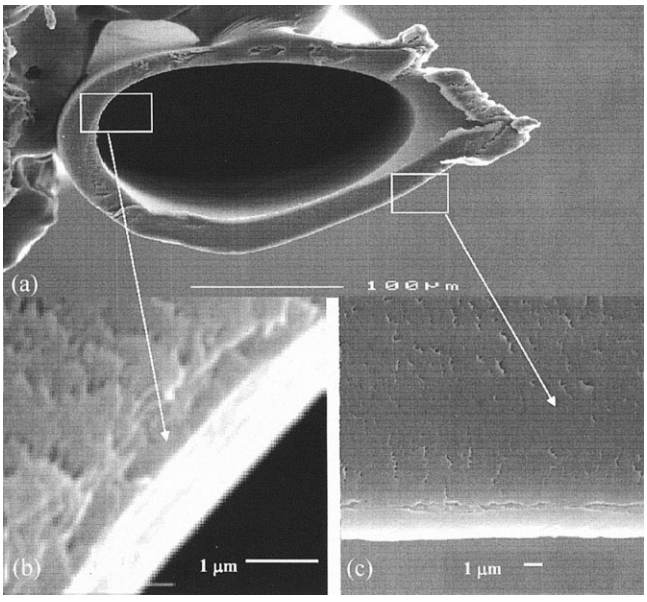

Figure 13 SEM images of (a) a cross section, (b) an internal skin layer, and (c) an external skin layer of a typical polysulfone dialysis hollow fiber.

CONCLUSIONS

The following conclusions were drawn from this work:

1. CAM, AFM, and SEM were successfully applied to the internal and external surfaces of dialysis hollow fiber membranes.
2. Valuable surface information was obtained by correlating the results obtained from CAM to those from AFM.
3. By increasing the drying time of polysulfone hollow fibers, the roughness parameter and contact angle increased whereas the nodule size and pore size decreased.
4. The contact angle was increased as the ratio of the roughness parameter to the nodule size was increased. This was probably attributable to the increase of the capillary pressure required to force the test liquid into the troughs created between the nodules.
5. A theoretical model capable of predicting the effect of the surface morphology on contact angle was developed. The theoretical prediction showed that the measured contact angle would be greater than the value intrinsic to the membrane material, and the prediction was confirmed by experimental data.
6. Blending of PEG with molecular weights of 1500 and 2000 Da in the spinning solution increased the roughness parameter and nodule size but decreased the contact angle, which improved the biocompatibility compared with blending of PEG with a molecular weight of 1000 Da.
7. According to SEM microstructure studies, the polysulfone dialysis hollow fibers used in this study have dense skin layers on both the interior and exterior surfaces. The ultrathin inner surface provided low resistance to solute permeability, which improved the separation performance,

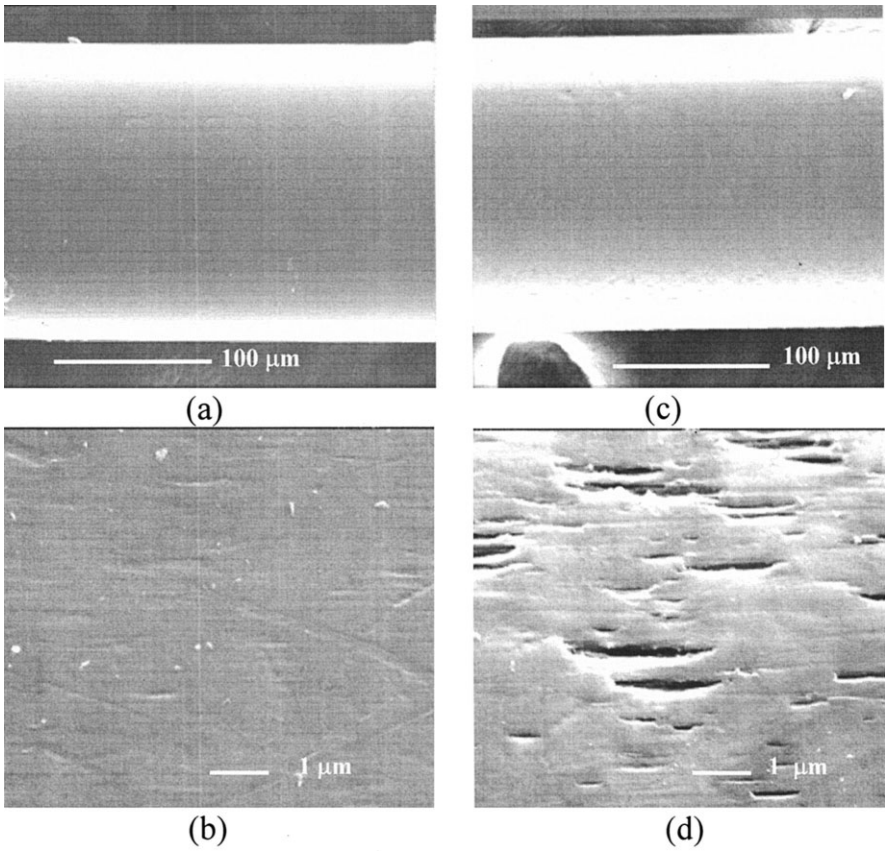

Figure 14 SEM images of the surfaces of polysulfone hollow fibers' (a) external surface after 5-min drying (scale bar = 100 μm), (b) external surface after 5-min drying (scale bar = 1 μm), (c) external surface after 1-h drying (scale bar = 100 μm), and (d) external surface after 1-h drying (scale bar = 1 μm).

whereas the outer thin layer acted as an excellent barrier to blood endoxins.

8. SEM microstructure studies also demonstrated that fissures and cleavages were generated at the hollow fiber external surfaces when they were dried for 1 h or longer.
9. The postfabrication drying period of polysulfone hollow fibers should be minimized (i.e., <1 h) because longer drying periods increased the surface roughness and hydrophobicity of the membrane, thereby generating fissures and cleavages on the external surfaces that may compromise membrane performance and biocompatibility.

The author is grateful to Baxter Healthcare Inc., Miami Lakes, FL, and the Government of Ontario, Canada, for supporting him under the Ontario Graduate Scholarship in Science and Technology.

NOMENCLATURE

Variables

D_n	nodule size (nm)
D_p	pore size (nm)
e_{coh}	cohesive energy of solid (J/m^3)
$f(x, y)$	surface function relative to the center plane (nm)
f_{SL}	fraction of the surface where solid and liquid are in contact
f_{LV}	fraction of the surface where liquid and vapor (air) are in contact
k	ratio of mean surface roughness to mean surface nodule size (R_a/μ_n)
L_x	surface dimension in x direction (nm)
L_y	surface dimension in y direction (nm)
R_a	mean surface roughness (nm)

Greeks

γ_{LV}	liquid–vapor surface tension (J/m^2)
γ_{SL}	solid–liquid surface tension (J/m^2)
γ_{SLE}	effective solid–liquid surface tension (J/m^2)
γ_{SV}	solid_–vapor surface tension (J/m^2)
μ_n	mean nodule size (nm)
μ_p	mean pore size (nm)
δ_{sp}	solubility parameter (J$^{1/2}$ m$^{-3/2}$)
σ_n	geometric standard deviation of nodule size
σ_p	geometric standard deviation of pore size

θ_a advancing contact angle (°)
θ_e equilibrium contact angle (°)
θ_i intrinsic contact angle (°)

References

1. Mulder, M. Basic Principles of Membrane Technology; Kluwer: Dordrecht, 1995.
2. Tsunoda, N.; Kokubo, K.; Sakai, K. ASAIO J 1999, 45, 418.
3. Tsai, M. Y.; Lin, J. C. J Biomed Mater Res 2001, 55, 554.
4. Palacio, L.; Calvo, J. I.; Pradanos, P.; Hernandez, A.; Vaisanen, P.; Nystrom, M. J Membr Sci 1999, 152, 189.
5. Chan, C. M. Polymer Surface Modification and Characterization; Hanser: New York, 1994.
6. Taniguchi, M.; Pieracci, J. P.; Belfort, G. Langmuir 2001, 17, 4312.
7. Mcluch, T. B.; Chiang, C. Y.; Jaanine, H.; Nguyen, T.; Radovich, J. M.; Ruzius, K.; Silva, L. K.; Washington, G. U.S. Pat. 6,218,441, B1, 2001.
8. Nguyen, T.; Ericsson, L. Althane Polysulfone Membranes Technical Information; Althin Medical: Miami Lakes, FL, 1999.
9. Good, R. J. In Contact Angle Wetting and Adhesion; Mittal, K. L., Ed.; Utrecht, The Netherlands, 1993; p 3.
10. De Bartolo, L.; Morelli, S.; Bader, A.; Drioli, E. J Mater Sci Mater Med 2001, 12, 959.
11. Singh, S.; Khulbe, K. C.; Matsuura, T.; Ramamurthy, P. J Membr Sci 1998, 142, 111.
12. Asmanrafat, M. M.S. Thesis, University of Ottawa, 2002.
13. Spelt, J. K.; Vargha-Butler, E. I. In Applied Surface Thermodynamics; Neumann, A. W.; Spelt, J. K., Eds.; Marcel Dekker; New York, 1996; p 379.